International Journal of Enhanced Research in Science, Technology & Engineering
ISSN: 2319-7463, Vol. 15 Issue 2, February-2026

A Study Of: Application of CFD in Studying Heat Transfer and Airflow in Natural Draft Cooling Towers

Himanshu Chaudhary

Assistant Professor Department of Engineering and Technology AISECT University, Hazaribag

ABSTRACT

Natural Draft Cooling Towers (NDCTs) constitute a highly efficient and widely adopted solution for heat rejection at the cold end of steam turbine cycles in large thermal and nuclear power plants. Their operation relies on buoyancy-driven airflow, evaporative cooling, and complex coupled heat- and mass-transfer processes between descending water films or droplets and ascending air streams. The overall thermal performance of an NDCT—particularly the attainable cold-water temperature—is strongly influenced by geometric configuration, construction details, fill type, and environmental conditions such as crosswinds. Owing to the inherently three-dimensional, turbulent, and multiphase nature of the internal flow field, traditional analytical models and large-scale experiments provide limited insight into the underlying aero thermal mechanisms. This study presents a comprehensive numerical investigation of airflow and heat transfer in natural draft cooling towers using advanced Computational Fluid Dynamics (CFD). The modeling framework couples three-dimensional turbulent flow simulation with local heat and mass transfer formulations and detailed cooling-water film calculations, enabling realistic representation of aerodynamic and thermodynamic behavior under specified operating conditions.

After rigorous validation against available experimental and operational data, the numerical approach is applied to assess the influence of critical design and operational parameters, including modern fill types, inner rim outlet structures, additional flue gas discharge, and various crosswind scenarios. Simulation results demonstrate that contemporary high-performance fill materials significantly enhance tower efficiency by increasing interfacial contact area and promoting effective evaporative cooling, thereby reducing outlet water temperature. Conversely, crosswind conditions induce asymmetric airflow distribution, recirculation zones, and plume deflection, leading to measurable degradation in thermal performance and elevated cold-water temperatures. Under unfavorable wind conditions, periodic ingestion of cold ambient air at the tower outlet may occur, resulting in unstable operating behavior and further efficiency losses.

The presence of an inner rim structure at the tower exit is shown to mitigate these adverse effects by stabilizing the outlet flow and suppressing recirculation phenomena. Additionally, simulations indicate that auxiliary flue gas injection can alter buoyancy forces and internal flow patterns, with implications for both performance enhancement and environmental impact. Overall, the study confirms that CFD provides a robust and comprehensive tool for predicting and optimizing NDCT performance, offering detailed insight into flow structures and thermal processes that are difficult to obtain experimentally. The findings highlight the critical importance of geometric design; fill technology, and environmental conditions in determining cooling effectiveness and operational stability. By enabling parametric evaluation and design optimization, CFD-based analysis supports the development of energy-efficient, reliable, and environmentally sustainable cooling systems for modern power generation facilities.

Keywords: CFD, Natural Draft Cooling Tower, Heat Transfer, Airflow, Evaporation, Multiphase Flow, Turbulence Modeling.

INTRODUCTION

Cooling towers are essential heat-rejection devices used to dissipate excess thermal energy from circulating cooling water systems to the atmosphere. Among the various types, natural draft cooling towers (NDCTs) are extensively employed in

large thermal and nuclear power plants due to their ability to operate without mechanical fans, thereby significantly reducing auxiliary power consumption and operational costs. NDCTs function on the principle of the chimney effect, in which warm, humid air inside the tower becomes less dense than the surrounding ambient air and rises upward under buoyancy forces.

This upward motion induces the inflow of cooler ambient air through the tower base. Heated water from the steam condenser is distributed through spray nozzles over fill materials, which greatly increase the interfacial area between water and air.

As the water descends through the fill, a portion of it evaporates, removing latent heat and thereby reducing the temperature of the remaining water before it is collected and recalculated. Cooling towers serve as the “cold end” of the steam turbine cycle in power plants. Their primary purpose is to provide sufficiently low cooling water temperatures to enable efficient condensation of exhaust steam from low-pressure turbines.

The condenser pressure is thermodynamically linked to the temperature of the cooling water supplied by the tower; lower cooling water temperatures result in lower condenser pressures, which in turn improve turbine efficiency and overall plant power output. Therefore, achieving cooling water temperatures as close as possible to ambient wet-bulb temperature is crucial for optimal cycle performance. Wet cooling towers typically achieve the highest efficiencies because they utilize both convective and evaporative heat transfer mechanisms.

In these systems, hot water from the condenser is cooled through direct contact with ambient air. The effectiveness of this process depends strongly on the contact time and surface area between air and water, which are enhanced by distributing the water over structured fill materials composed of grids, bars, or plates. As water trickles downward through the fill, cooling occurs via two simultaneous processes. First, a fraction of the water evaporates, extracting latent heat from the remaining liquid. Second, sensible heat is transferred from the water to the air through convection.

Together, these processes produce significant temperature reduction. Natural draft cooling towers represent one of the most efficient designs, although they require substantial construction costs due to their large size. Their operation relies entirely on buoyancy-driven airflow rather than mechanical assistance. Two principal flow configurations are commonly used: counter flow, in which air moves upward opposite to the descending water flow, and cross flow, where air flows horizontally across the falling water.

In contrast, mechanical draft cooling towers use fans to force air through the fill. Although mechanical systems achieve higher air velocities and enhanced heat transfer, they are typically smaller in size but consume electrical power, which reduces net plant efficiency. Modern NDCTs are massive structures, often exceeding heights of 200 meters with base diameters around 150 meters. Advanced designs may incorporate features such as central flue gas discharge systems to integrate power plant exhaust flows with cooling tower operation.

These geometric and structural characteristics strongly influence aerodynamic performance, internal flow distribution, and thermal efficiency. Despite their advantages, natural draft cooling towers are highly sensitive to operating and environmental conditions. Additional flue gas discharge can alter buoyancy forces and internal temperature fields, while external factors such as crosswinds can significantly distort airflow distribution. Under crosswind conditions, incoming air may be unevenly distributed across the fill region, leading to asymmetric cooling performance and potential recirculation zones.

Moreover, the buoyancy-driven airflow within the tower can be disrupted by the entrainment of cooler ambient air at the outlet, which may result in reduced efficiency or unstable operating behavior. Given the scale and complexity of these phenomena, understanding the aero thermal behavior of NDCTs requires advanced analytical tools capable of capturing three-dimensional turbulent flow, coupled heat and mass transfer, and multiphase interactions. This necessity has motivated the widespread adoption of Computational Fluid Dynamics as a primary method for performance analysis and design optimization of modern cooling towers.

Fig. 1. Schematic of a natural draft cooling tower.

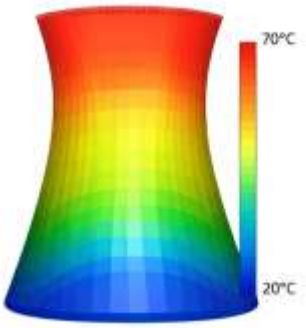

Fig. 2. CFD temperature distribution inside the tower.

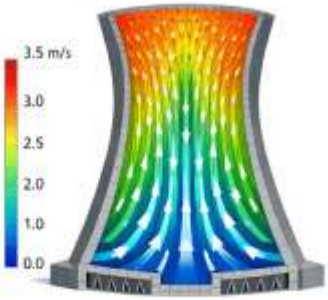

Fig. 3. Velocity vectors of buoyancy-driven airflow.

Fig. 4. Effect of crosswind on plume dispersion.

Figures 1–4 collectively illustrate the fundamental aero thermal processes, internal flow behavior, and environmental influences governing the performance of a natural draft cooling tower (NDCT).

Figure 1 presents a schematic representation of a natural draft cooling tower, highlighting its principal components and operating mechanism. Hot water from the condenser enters the tower near the top and is distributed through spray nozzles over the fill section, which provides a large surface area for heat and mass transfer. As the water trickles downward through the fill, it comes into direct contact with upward-moving air drawn from the base openings. A portion of the water evaporates, extracting latent heat from the remaining liquid. Drift eliminators prevent excessive water loss by capturing entrained droplets, while the cooled water collects in the basin at the bottom for recirculation. Simultaneously, warm, moisture-laden air rises and exits the tower as an exhaust plume due to buoyancy forces.

Figure 2 illustrates the temperature distribution within the tower predicted by Computational Fluid Dynamics (CFD). The color gradient indicates a transition from cooler regions near the air inlets at the base (approximately 20 °C) to significantly warmer zones toward the upper section (up to about 70 °C), where heated, humid air accumulates before discharge. This vertical temperature stratification demonstrates the effectiveness of evaporative cooling and the development of buoyancy forces that drive natural convection. The figure also highlights the non-uniform temperature field across the tower cross-section, which arises from complex interactions between airflow, water distribution, and structural geometry.

Figure 3 shows velocity vectors representing buoyancy-driven airflow inside the tower. Air enters through the base openings with relatively low velocity, accelerates as it passes through the fill region due to heating and density reduction, and forms a strong upward flow toward the outlet. The vector pattern reveals three-dimensional flow structures, including regions of accelerated core flow and potential recirculation near the walls. These features are critical because they directly influence local heat transfer rates, evaporation intensity, and overall cooling performance.

Figure 4 demonstrates the effect of crosswind on plume dispersion and tower operation. External wind causes deflection of the exhaust plume and introduces asymmetry in the airflow entering the tower. Under strong crosswind conditions, air distribution across the fill becomes uneven, leading to localized regions of reduced cooling efficiency. In severe cases, cold ambient air may be entrained from the top into the tower interior, disrupting the buoyancy-driven flow and causing distorted heat transfer patterns. Such phenomena increase the outlet water temperature and reduce the efficiency of both the cooling tower and the associated steam turbine cycle.

Together, these figures emphasize that NDCT performance depends not only on internal heat and mass transfer processes but also on geometric design features and external environmental conditions. Accurate prediction of these complex interactions requires comprehensive three-dimensional numerical modeling using advanced CFD techniques. By capturing temperature fields, velocity distributions, and plume behavior under varying operating scenarios, CFD enables detailed assessment of tower efficiency and supports the development of optimized, stable, and energy-efficient cooling tower designs.

2 Numerical modelling

2.1 Implementation of a heat transfer and mass transfer model

The water-side and air-side flow in a wet cooling tower is a two-phase flow with complex heat transfer and mass transfer conditions between both fluids. Thus, the complete numerical simulation of all relevant conservation equations for the three dimensional flow in cooling towers is still beyond the economical application for industrial use with respect to time and cost efforts. Therefore, a simplification is introduced by handling the wet air as a one-phase mixture of fluids consisting of the two components (1) dry air and (2) water steam. This is necessary to take into account the change in density due to the local wetness. In the following section, this one-phase model fluid is mentioned as “air” or “air-side.”

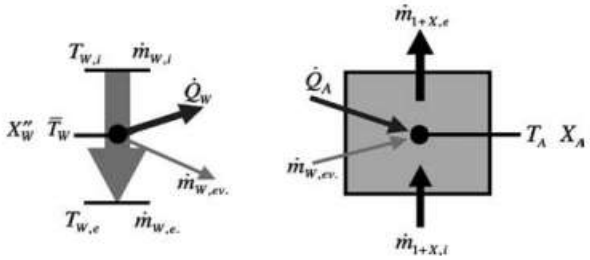

Figure 3: Physical parameters for heat and mass balances at a cooling water element (left) and a finite volume cell of the air-side (right).

Saturated altogether, the local heat flux transferred from the cooling water element can be calculated as follows:

$$Q_W = a \cdot A \cdot (T_W - T_A) + \beta_x \cdot A \cdot (X''_W - X_A) \cdot \Delta h_{ev} \qquad (1)$$

In case the air in the fi nite volume cell is saturated with water as well as the air in contact to the cooling water fi lm, but a temperature gradient between the cooling water fi lm and the air-side is established, the diffusion process continues further despite the saturated air condition due to the gradient of the water content. This leads to a re-condensation of water on the air-side. The re-condensed water and small droplets taken away by mechanical forces are the reason for the visible plume at the cooling tower exit. The re-condensation of steam on the air-side is not part of the used numerical models up to now.

The outlet temperature of the cooling water for the cooling water element can be calculated based on the fi rst law of thermodynamic as following:

$$T_{W,e} = \frac{\left(\dot{m}_{w,i} \cdot c_W \cdot T_{W,i} - \dot{Q}_W - \dot{m}_{W,ev} \cdot c_W \cdot \bar{T}_W\right)}{\dot{m}_{W,e} \cdot c_W} \qquad (2)$$

The heat flux into the air-side finite volume cell is mainly determined by the convectively transferred heat:

$$\dot{Q}_A = a \cdot A \cdot (\bar{T}_W - T_A) + \dot{m}_{W,ev} \cdot h''_S \qquad (3)$$

2.2 Evaporation number and Lewis analogy The theoretical approach on the calculation of local mass transfer and heat transfer is mainly based on an evaporation number kV (often also mentioned as Merkel number) for the determination of a mass transfer coefficient and the Lewis analogy for determination of a convective heat transfer coefficient.

2.2 The Merkel number is defined:

$$k_V = Me = \int_A \frac{\beta_x \, dA}{\dot{m}_W} \qquad (4)$$

The manufacturers of the cooling tower fills provide the information on the dependency of the Merkel number on the ratio λ of the dry air mass flow and the cooling water flow in their characteristic curves for the product:

$$Me = Me_{(\lambda=1)} \cdot \lambda^m \qquad (5)$$

In Anglo-Saxon countries, the following nomenclature is often used for the description of the fill characteristics curves:

$$\frac{KaV}{L} = f(L/G) = f(1/\lambda) \qquad (6)$$

Therefore, it is the responsibility of the manufacturer to provide the designer with precise fill characteristics for the thermal performance of the fills based on high quality measurements within special testing facilities by application of relevant test conditions for real operation.
The convective heat transfer coefficient is calculated based on the Lewis analogy taking into account a correction for one-directional diffusion at the phase interface [6]:

$$\frac{a}{\beta_x} = c_{pm} \cdot Le^{(1-n)} \cdot \frac{\left(p''_{S,W} - p_{S,A}\right)}{\left(p - p''_{S,W}\right) \cdot \ln\left(p - p_{S,A}/p - p''_{S,W}\right)} \qquad (7)$$

Here, c_{pm} is the specifi c heat capacity of wet air related to the dry air mass:

$$c_{pm} = c_{p,A} + c_{p,S} \cdot X_A \qquad (8)$$

The Lewis number and the exponent n depend on the flow type and are based on experimental investigations. The determination of the values for the investigated cooling tower is reported in Section 3.2.1.

For cooling tower performance calculations with conventional schemes, it is of great importance to calculate precisely the demand curve of the cooling tower, which depends on the specific design data of the cooling tower. The point of intersection of the demand curve and the cooling fill characteristic curve gives as a result the design value for the ratio λ as shown in Fig. 4. As the precise calculation of the cooling tower demand curve is a very difficult task because of the great number of influence parameters and the complex interaction of the cooling tower aerodynamics and thermodynamics, there is a great uncertainty within this approach.

The great advantage of the presented comprehensive numerical approach is that in a converged solution, the calculated operating points will automatically fulfill the necessary requirements. The inlet air mass flow is the result of the numerical simulation and it depends on the iterated heat transfer (based on the correlations), the pressure drop (based on further correlations), the cooling tower geometry, ambient conditions and inlet water flow conditions. The numerical results provide not only the integral values for transferred heat and the cold water temperature, but also the local data for the flow field, local heat and mass transfer values and local cooling down of the cooling water film. When the numerical model has been validated for a specific cooling.

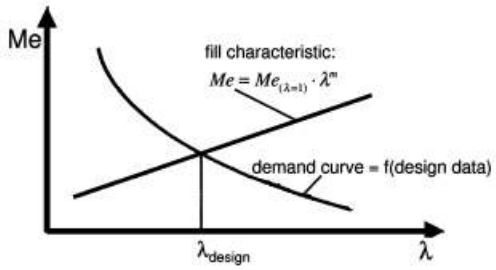

Figure 4: Conventional design approach based on characteristic curve and separated calculation of the cooling tower demand curve.

Tower, parametric studies on the variation of the ambient conditions (e.g. ambient temperature, pressure and humidity) from the design values allow a precise determination of the effects for the cooling tower performance, e.g. the calculated cold water temperature. This includes cross wind situations or installation of different fill types or change of the fill arrangements. Another topic of interest might be an inhomogeneous distribution of the sprayed water instead of a homogeneous distribution. Thus, designers and operators of cooling towers get an improved decision basis for new cooling tower arrangements or retrofit measures for existing cooling towers 3 Validation 3.1 Aerodynamic code validation Based on

experimental results [7, 8] for the aerodynamics of a cooling tower model, the validation of the basic CFD code has been performed. The original cooling tower has a total height of H tot = 120 m, a waist height (smallest diameter) of Hw = 0.79Htot, and a base diameter of Db = 100 m. In the experiments, the geometry model of the cooling tower has a scaling factor of 1:275. For aerodynamic investigations of a group arrangement, further experiments include an additional cooling tower model that has been placed at a distance of d = 1.87Db behind the first model. The contour of the cooling towers has been modeled by a circular arc that can be derived from the given geometric parameters. The three-dimensional grid consists not only of the cooling tower; it is also necessary to model the environment of the cooling tower with boundaries far away from the cooling tower such that undisturbed pressure distributions can be prescribed, which, under these conditions, have only a negligible influence on the calculated pressure distributions of the cooling tower. Here, all boundaries of the three-dimensional grid in all three coordinate directions have been placed at least at a distance of three times the base diameter away from the cooling towers. Figure 5 shows a close-up of the numerical grid of the cooling tower. The grid for the external flow part consists of approximately 550,000 finite volume cells. The internal flow region of the cooling tower that consists also of the air supply channel and a diffuser has been modeled with approximately 600,000 additional cells. Furthermore, the pressure losses of two sieves, one placed at the diffuser outlet and the other one placed in front of the tower waist have been taken into account by a pressure loss model based on pressure loss coefficients.

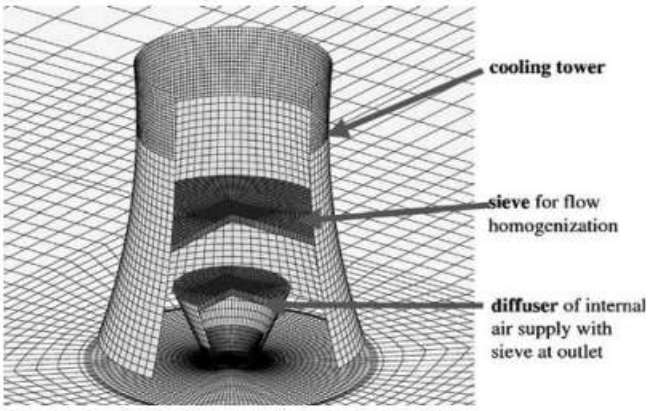

Figure 5: Numerical model and grid of single cooling tower.

A fully turbulent flow has been reached in the experiments by additional turbulators on the surface of the cooling tower. Thus, the standard-k, ε-model with an additional wall roughness parameter has been used in the numerical simulations. Furthermore, calculations with the original geometry size have been performed. In that case, the flow has a very high Re number and a turbulent boundary layer is established. Therefore, the calculations can be performed with a hydraulic even surface, means without an additional roughness parameter.

For the cross wind simulation, a velocity profile has to be prescribed at the inlet boundary, which should be an approximation of the atmospheric boundary layer. This is reached by a velocity distribution in dependency of the atmospheric height z in the following exponential law [8]:

$$\frac{c(z)}{c_\infty} = \left(\frac{z}{z_\infty}\right)^{0.25} \qquad (9)$$

In the investigated cases of a single cooling tower and a group arrangement of two cooling towers, the undisturbed velocity c∞ at the height of the cooling tower exit has been c∞ = 2.2 m/s.

3.1.1 Results for single cooling tower

Based on the measured pressure distribution (timely averaged values) on the cooling tower surface at the waist height of 0.79Htot, a comparison of the pressure coeff cients

$$\frac{c(z)}{c_\infty} = \left(\frac{z}{z_\infty}\right)^{0.25} \qquad (9)$$

with the calculated values can be given in Fig. 6

The values are displayed in polar coordinates. The 0°-position is the stagnation point of the cooling tower. Measured values are available for the hydraulic even and hydraulic rough surfaces. It can be shown that the calculated pressure distribution is in good agreement with the measured values in both cases.

3.1.2 Results for cooling tower arrangement

The numerical grid is shown in Fig. 7. The arrangement of the cooling towers has been exposed to a cross wind with an offset angle of 15° to the centre connection line of the cooling towers. Thus, an asymmetric velocity and pressure distribution can be expected. This can be seen in the calculated pressure fields in Fig. 8a and b. Whereas Fig. 8a shows the experimental case with a rough

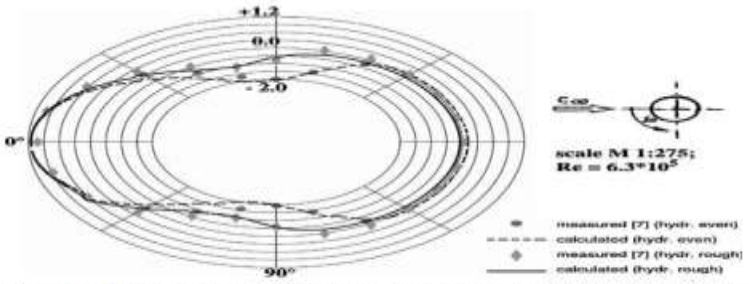

Figure 6: Distribution of c_p-values on the cooling tower surface (single tower) at a height of $0.79H_{tot}$.

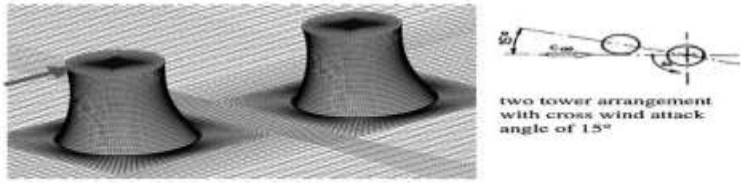

Figure 7: Numerical model and grid of two-tower arrangement.

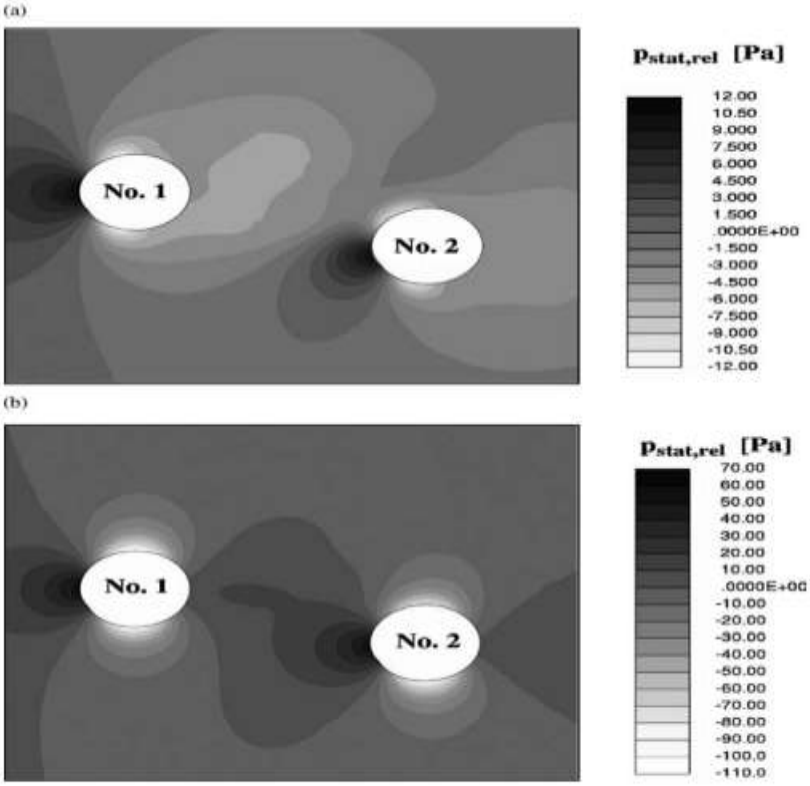

Figure 8: Calculated static pressure fields of the group arrangement at a height of $0.79H_{tot}$: (a) hydraulic rough surface, scale M 1:275, Re = 6.3×10^5; (b) hydraulic even surface, scale M 1:1, Re = 4.327×10^7.

Surface, Fig. 8b shows the pressure field by taking into account the original cooling tower size and a hydraulic even surface. From the significant differences in the pressure field, it can be concluded that the experimental results cannot be transferred to the real flow situation. Due to the limitation of the established Re number, aerodynamic interaction phenomena are overestimated in the experimental case.

With respect to the aerodynamic validation purpose, the comparison of the measured and calculated pressure coefficients for the second cooling tower in Fig. 9 shows a good agreement. It can also be seen that for the realistic very high Re number situation, there are significant differences in the distributions that are showing the reduced effect of the front cooling tower on the second one.

3.2 Validation of the coupled aero thermodynamic and heat transfer model

As the major purpose of the numerical investigation has been to get detailed results on the interaction of the cooling tower aerodynamics, thermodynamics and heat transfer, the basic models as described in Section 2 have been implemented to the code. Thus, it has been necessary to validate the code and models by comparison of the calculated data with results of a counter flow cooling tower that have been available from the operator of a power plant. Initial calculations for the validation purpose are without cross wind effects.

3.2.1 Numerical model and boundary conditions

Basic geometry parameters of the investigated cooling tower are a total height of H to t = 117 m, a waist diameter of Dw = 61.3 m at a height of Hw = 90.7 m. Base diameter of the cooling tower is Db = 92.8 m. A three-dimensional half-grid with symmetry condition has been generated for the cooling tower (Fig. 10). The half grid contains approximately 500,000 cells. In the internal part of the cooling tower,

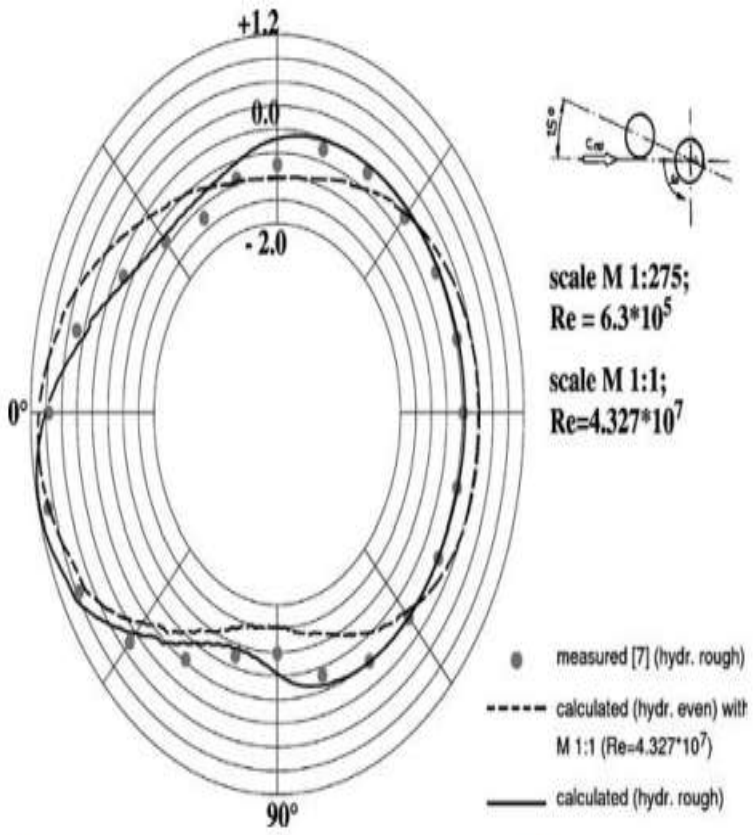

Figure 9: Distribution of c_p-values on the second cooling tower surface (group arrangement) at a height of $0.79H_{tot}$.

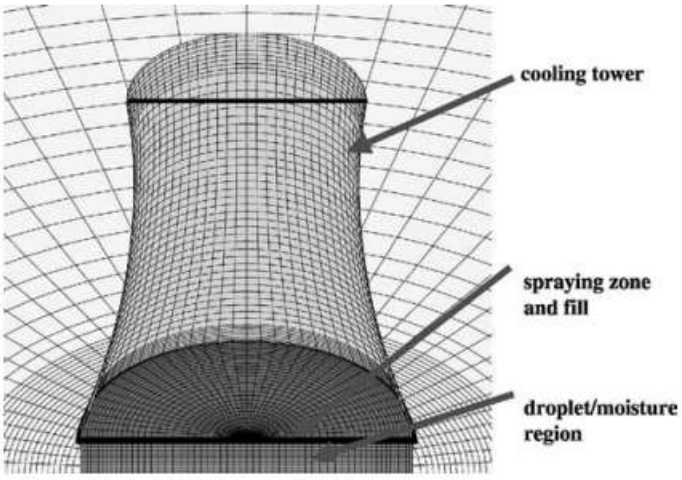

Figure 10: Numerical grid for coupled aerothermodynamic and heat transfer calculation (3D view into the tower).

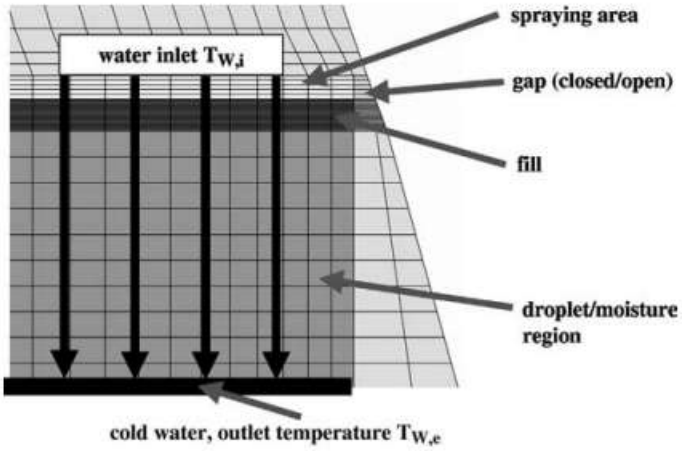

Figure 11: Detailed model description of the internal part of the cooling tower.

high-grid density modeling of the spraying zone, the fill volume, and the droplet/ moisture region has been used as it can be seen in the zoomed area of Fig. 11. The correlations of the evaporation number kV (Me number) are needed for the heat transfer and mass transfer calculation in the spraying zone, fill volume and droplet/moisture region. Here, the necessary input has been provided by manufactures of the fill and by the power plant operators. In the investigated case conditions, the fill type of the cooling tower is fibrated concrete that has been replaced by a plastic fill type (see Section 4.1). For the fill type, the following correlation in dependency of the local mass flow ratio λ can be given:

$$k_{V,fill} = 1.22 \cdot \lambda^{0.67} \qquad (11)$$

For the spraying zone and droplet/moisture area, the following correlations have been used:

$$k_{V,spray} = 0.15 \cdot \lambda^{0.67} \qquad (12)$$

$$k_{V,drop} = 0.03 \cdot \lambda^{0.67} \qquad (13)$$

Based on the work provided by Poppe [6] the value of the Le number is Le = 0.865 and the exponent n in the Lewis analogy has a value of n = 0.33. Whereas an exponent of n = 1.0 is valid for a fully turbulent flow, a value of n = 0.33 indicates a flow with beginning thermal and hydrodynamic boundary layer formation. For the Lewis number, a value of Le = 0.865 is valid in a wide temperature range.

Furthermore, the pressure loss coefficients for the different regions have to be provided. These values have been provided by the designers of the cooling tower and the manufactures of the fill elements. Thus, these values depend on the specific design of the cooling tower. As precise values are part of the companies' proprietary, it is necessary to contact the manufactures so that such values can be provided. Here, the pressure loss coefficient for the fill elements itself is also dependent on the local fl ow velocity of the humid air. For velocities from v = 1 m/s to v = 2.5 m/s the loss coefficient is decreasing from $\zeta = 18$ to $\zeta = 10.8$. For the moisture/droplet region loss coefficients from $\zeta = 21.1$ for v = 1 m/s to $\zeta = 12.6$ for v = 2.5 m/s can be provided. For the spraying zone the values for the loss coefficients are $\zeta = 7.03$ for v = 1 m/s to $\zeta = 4.2$ for v = 2.5 m/s.

Finally, some basic thermodynamic data for the cooling tower operation are needed as input data (boundary conditions). These values are the air pressure (p0 = 1013.0 hPa), the air temperature (TA = 282.65 K), humidity ($\phi = 77.17\%$), water inlet temperature ($T_{W,i}$ = 307.35 K), and the water mass flow (mW,i = 58500.0 t/h). Due to the huge size of the cooling tower, the atmospheric layering of pressure and temperature as a function of the height has to be taken into account at the far field boundaries of the grid. The dry air mass flow (mA,dry) and the cold water temperature ($T_{W,e}$) are results of the numerical simulation. Thus, the local mass flow ratio Λ distribution will be also a calculation result at the end of the numerical iteration process. Of course, the local velocity field, local heat fluxes, and local mass fluxes are also a result of the CFD analysis. Thus, the great advantage of this comprehensive CFD approach is not only the precise calculation of the integral result values of the cooling tower but also the inclusion of several influences on these values for a systematic investigation on the improvement potential.

3.2.2 Aero thermodynamic calculation results The calculated cold water temperature is the most critical parameter with respect to the calculated performance of the cooling tower. Initially, the temperature values for the water-side of the simulation have been set equally to $T_{W,i}$ = 307.35 K, that is the inlet warm water temperature. During the iteration process, the calculated cold water temperature decreases with ongoing calculation with only few numerical instability. This has been documented by the graph in Fig. 12, which shows the calculated cold water temperature during the iteration process. Finally, a converged value of TW,e = 295 K has been reached after 1500 steps with only minor further change. The fi nal calculation value TW,e = 294.96 K is very close to the target design value of 294.75 K and clearly within a confi dence level of ±0.5 K requested by the cooling tower designers. Table 1 lists the most important integral values of the numerical simulation. The comparison of the total transferred heat shows that there is only a 1.8% difference.

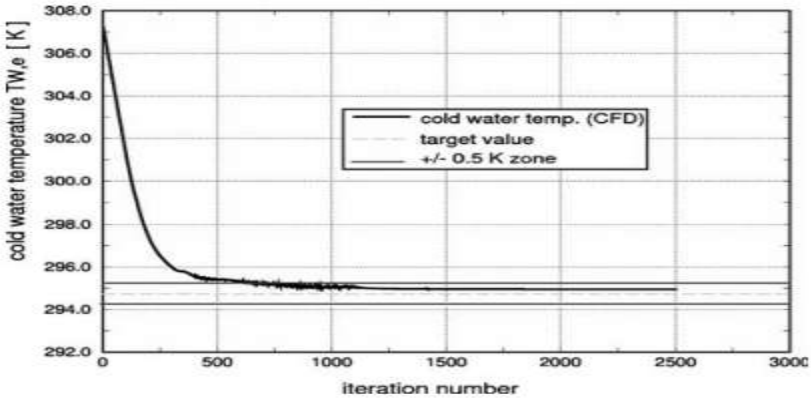

Figure 12: Cold water temperature calculation.

Table 1: Integral results on transferred heat and mass flow.

	Calculation		Design point
Cold water temperature	294.960 K		294.750 K
Total heat (transferred from water)	835.87 MW		850.0 MW
Convective heat	226.74 MW	27.13%	
Evaporation heat	609.13 MW	72.87%	
Total transferred heat in spraying area	76.75 MW	9.18%	
Total transferred heat in fill region	577.51 MW	69.09%	
Total transferred heat in droplet region	181.61 MW	21.73%	
Evaporated water mass flow	246.98 kg/s	1.52%	
Dry air mass flow	13779 kg/s		13390 kg/s
Averaged cooling tower outlet temperature	298.93 K		

Between the value obtained from calculation and the cooling tower design value of 850 MW. The dry air mass flow is only 2.9% higher than the design value, which is also an acceptable deviation as the dry air mass flow is a calculated value based on the full aerothermodynamics and not a boundary condition.

Based on the local values in the flow field, one can distinguish precisely between the transferred convective heat and the evaporation heat, which is the major part (72.87%) of the heat transferred from the water side. Furthermore, it can be distinguished between the heat transferred in the spraying area, the fill, and the moisture/droplet region (Table 1). The evaporated water mass flow is 246.98 kg/s (1.52% of inlet water mass flow).

The flow visualization by flow vectors in a two-dimensional sectional cut is presented in Fig. 13. The dry air is sucked into the tower at the bottom and then turned into vertical direction so that only a minor part of the air streams through the complete droplet/moisture region until the centre of the tower. Then, the fl ow direction is homogenized in the fi ll area by the fi ll installation. Maximum fl ow velocities in the centre region of the tower are approximately 8 m/s. Furthermore, it can be seen in the zoomed region (Fig. 13b) that for the stationary case and without side wind effects no cold air entry in the tower exit area close to the tower rim can be observed.

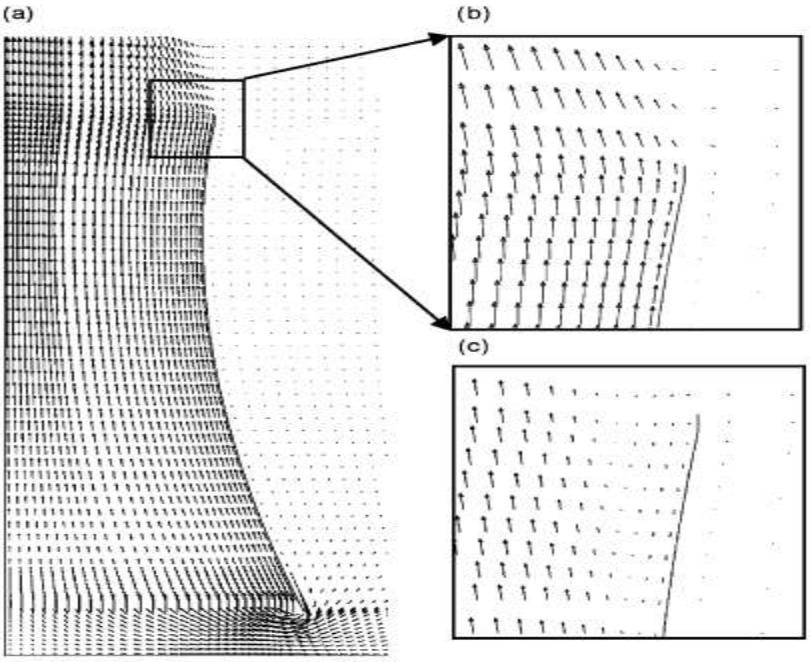

Figure 13: Cooling tower flow field: (a) flow vectors; (b) detail of outlet flow (closed gap); (c) detail of outlet flow (open gap).

The situation is different in the case, if the circular gap, as indicated in Fig. 11, is opened in the calculation model. In that case (Fig. 13c), a part of the inlet air is able to flow through the gap and leads to a low kinetic boundary layer flow. As a result, some part of the environmental cold air is able to generate a partly blockage of the tower outlet area close to the tower rim. A recalculating area of cold air can be observed. Overall performance of the cooling tower is significantly reduced. The simulation underlines the importance of the typical design feature to close gaps in the fill area near to the cooling tower wall.

4 Influences on the cooling tower performance

Based on the validation calculation of the cooling tower as shown in Section 3.2, the influence of several design features on the cooling tower performance is investigated by application of the numerical method.

4.1 Different fill types

With respect to the calculations for validation (reference case), the fill type has been fibrated concrete. It has been replaced by a modern plastic fill type as shown in Fig. 14 for an example. Such modern fill types are characterized by an improved heat transfer, low pressure losses and a high life-span. The correlations of the evaporation number kV are needed for the new fill type. The following correlation in dependency of the local mass flow ratio λ can be given:

$$k_{V,fill} = 1.92 \cdot \lambda^{0.633} \quad (14)$$

For the spraying zone and droplet/moisture area, the following correlations have been used:

$$k_{V,spray} = 0.15 \cdot \lambda^{0.633} \quad (15)$$

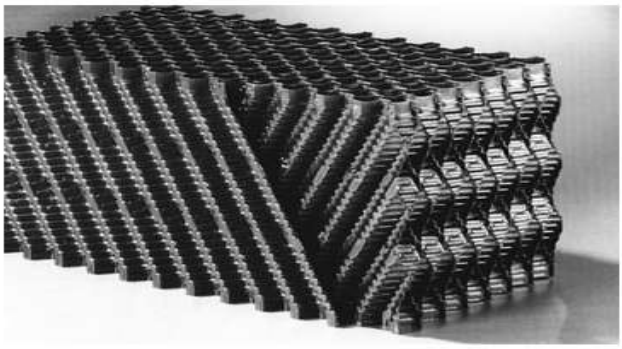

Figure 14: Typical plastic fill element for cooling tower application.

$$k_{V,drop} = 0.03 \cdot \lambda^{0.633} \quad (16)$$

Furthermore, the pressure loss coefficients for the different regions have to be provided. The pressure loss coefficient for the fi ll elements itself is dependent on the local flow velocity of the humid air. For velocities from v = 1 m/s to v = 2.5 m/s the loss coefficient is decreasing from ζ = 19.25 to ζ = 11.52. For the moisture/ droplet region loss coefficients and the spraying zone, the same pressure loss coefficients have been applied as for the reference calculation (see Section 3.2.1).

Whereas the environmental conditions in the calculation are the same as in the reference case, some operating parameters have been changed (Table 2). The water inlet temperature is $T_{W,i}$ = 306.05 K, and the inlet water mass flow mW = 63,000.0 t/h (17500 kg/s). Initially, the temperature values for the water-side of the simulation have been set equally to TW,i = 306.05 K, that is the inlet warm water temperature. During the iteration process, the calculated cold water temperature decreases with ongoing calculation and shows again an excellent convergence behaviour. That has been documented by the graph in Fig. 15. Finally, a converged value of

Table 2: Comparison of the operating conditions.

	Plastic fill type	Fibrated concrete fill type
Environmental temperature	282.65 K	282.65 K
Humidity	77.17%	77.17%
Environmental air pressure	1.013 bar	1.013 bar
Water inlet temperature	306.05 K	307.35 K
Inlet water mass flow	17500 kg/s	16250 kg/s

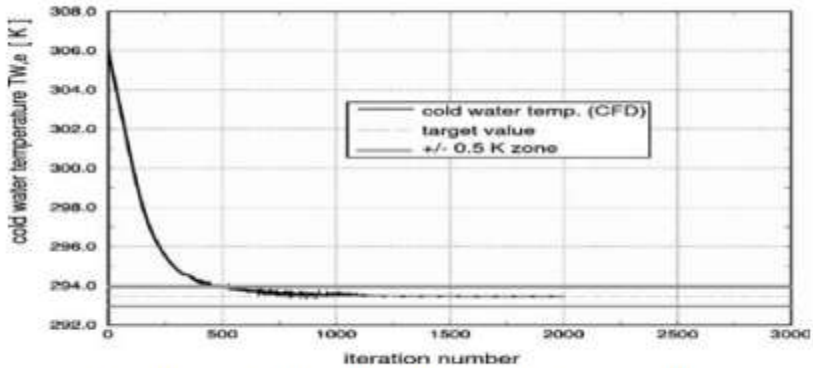

Figure 15: Cold water temperature calculation.

Table 3: Integral results on transferred heat and mass flow.

	Calculation		Design point
Cold water temperature	293.455 K		293.450 K
Total heat (transferred from water)	914.35 MW		915.0 MW
Convective heat	252.63 MW	27.63%	
Evaporation heat	661.72 MW	72.37%	
Total transferred heat in spraying area	55.60 MW	6.08%	
Total transferred heat in fill region	699.51 MW	76.50%	
Total transferred heat in droplet region	159.24 MW	17.42%	
Evaporated water mass flow	267.90 kg/s	1.53%	
Dry air mass flow	14137 kg/s		13230 kg/s
Averaged cooling tower outlet temperature	300.28 K		

$T_{W,e}$ = 293.455 K has been reached. That is almost identical to the design value (Table 3) and, therefore, clearly within a confidence level of ±0.5 K requested by the cooling tower designers.

Table 3 also lists the most important integral values of the numerical simulation. The comparison of the total transferred heat shows that this value is also almost identical to the design value of 915 MW. Compared to the reference case this means a significant increase in total heat transferred within the cooling tower (+7.6%). Thus, this improvement has a significant effect on the thermal efficiency of the steam cycle in the power plant. However, the percentage distribution of the heat transferred in the different regions of the cooling tower has only minor changes. The calculated dry air mass flow is approximately 6.8% higher than the design value.

One of the great advantages of the CFD approach is that detailed information on the local flow field is available. As an example, Fig. 16 shows the velocity distributions along section lines at different heights in the cooling tower. Thus, it can be shown that different velocity distributions are predicted for the different fill types. This is especially the case for the outlet distribution. For the simulation with plastic fill type, the bulk velocity is reduced, whereas the higher velocities close to the tower walls will lead to an increased kinetic energy in the boundary layer flow. That is of advantage with respect to the danger of local recirculation in the region of the cooling tower rim.

5. Cross wind effects on the cooling tower performance:

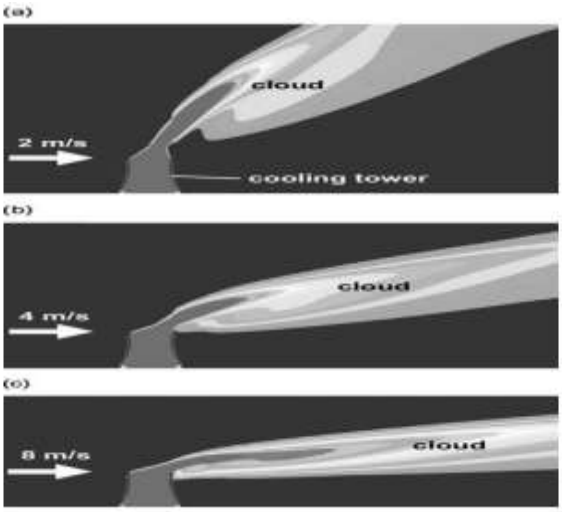

Figure 16: Temperature distributions for visualization of the cooling tower cloud propagation under cross wind effects: cross wind velocity of (a) 2 m/s, (b) 4 m/s and (c) 8 m/s.

well known that the interaction of the cooling tower flow and the cross wind can lead to a situation with a large region of cold air entering the tower exit. This phenomenon leads to a reduction in the effective cooling tower outlet area and, thus, has also a significant negative impact on the cooling tower performance and, furthermore, on the steam cycle performance. Thus, such operating situations have to be avoided or at least to be reduced in size by a modern design of the cooling tower.

6. Stable configurations

The modeling of the cross wind is done in the same way as described in the Section 3.1 for the aerodynamic validation. The cooling tower model that has been used contains the plastic fill type, the inner rim structure and a closed gap between the fill and the tower wall. Calculations (three-dimensional) have been performed with different wind velocities of vw = 2 m/s, vw = 4 m/s, vw = 8 m/s, and vw = 14 m/s. Figure 16 a–c shows the propagation of the cooling tower cloud due to the impact of different wind velocities. For all velocities, a stationary solution has been reached as shown in Fig. 16a–c. Therefore, the numerical simulations do not show any hint for a cold air ingestion at the tower exit. Nevertheless, an impact on the cooling tower performance, i.e. the cold water temperature, can be found as described by Fig. 17. For very small cross wind velocities of approximately vw = 2 m/s a slight improvement, i.e. a reduction of the cold water temperature can be observed. With further increasing cross wind velocities, there is a significant negative effect on the cooling tower performance and the cold water temperature increases. As it is shown by the curve in the diagram of Fig. 17, the increase in the cold water temperature is not linear but follows a parabolic shape and the situation worsens for high cross wind velocities. However, cold air ingestion is even not observed for the highest investigated cross wind velocity of vw = 14 m/s. The reasons for the stable behavior of the cooling tower can be found in the advantageous tower design. As it has been shown in Section 4.2, the inner rim structure has a stabilizing effect on the flow regime near to the tower rim. Furthermore, the plastic fi ll type leads to a boundary layer flow with a higher kinetic energy (see Section 4.1). Altogether, these two design features lead to a stable flow situation at the tower outlet even in a cross wind situation of up to vw = 14 m/s.

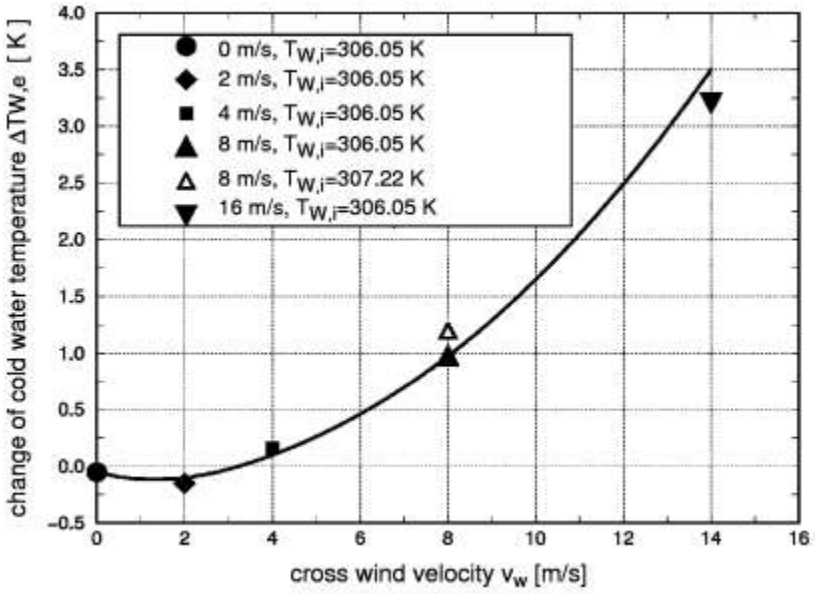

Figure 17: Calculated change of cold water temperatures for different cross wind velocities.

5.2 Unstable configuration with cold air ingestion Based on the understanding of the positive effects of the inner rim structure and the plastic fill type on the exit flow of the cooling tower, a more unstable situation has been expected for a cooling tower simulation without the inner rim structure and the fibrated concrete fill type. Furthermore, the gap between the fill and the tower wall has been opened in the numerical model as investigations presented in Section 3.2.2 have shown that an open gap leads to a recirculating flow area at the tower rim even in the case without cross wind. The three-dimensional simulation has been started based on the case without cross wind as the initial flow and temperature field and with a low cross wind velocity of vw = 2 m/s. Figure. 18 shows the calculated cold water temperature during the iteration process. Whereas in other simulation a good convergence has been observed, the situation is now different. A convergence of the cold water temperature has not been reached. Instead, there is a periodic fluctuation of the cold water temperature with the time steps. Figure 19 shows the visualization of the temperature field at four different time steps as indicated in Fig. 18. At position 1 (Fig. 19a), there is a low cold water temperature and there is only a minor area of cold air ingestion

near to the tower rim. Then, with increased cold air ingestion as shown in Fig. 19b for position 2, the cold water temperature increases rapidly. It reaches its maximum at position 3. Figure 19c shows for that case that a major part of the tower outlet is blocked by cold air. However, warm air in the lower part of the tower has started to push the cold air towards the outlet. Figure 16 shows a three-dimensional view of the temperature distributions for position 2 and position 3. Thus, it becomes even more obvious how deep the cold air can penetrate into the interior of the cooling tower.

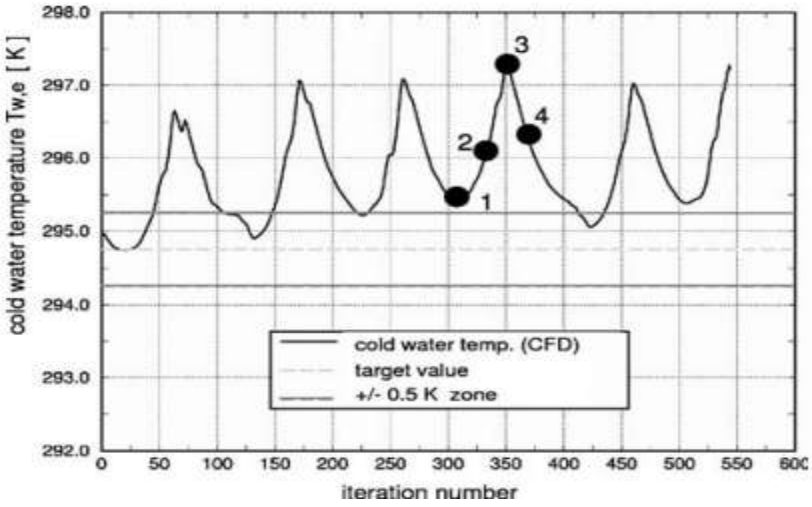

Figure 18: Cold water temperature calculation, cross wind velocity 2 m/s, cooling tower without inner rim structure.

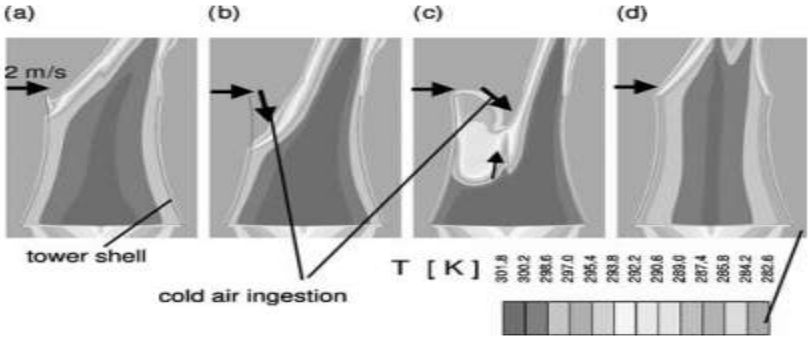

Figure 19: Temperature distribution at indicated iteration steps, cross wind velocity 2 m/s, cooling tower without inner rim structure: (a) position 1, (b) position 2, (c) position 3 and (d) position 4.

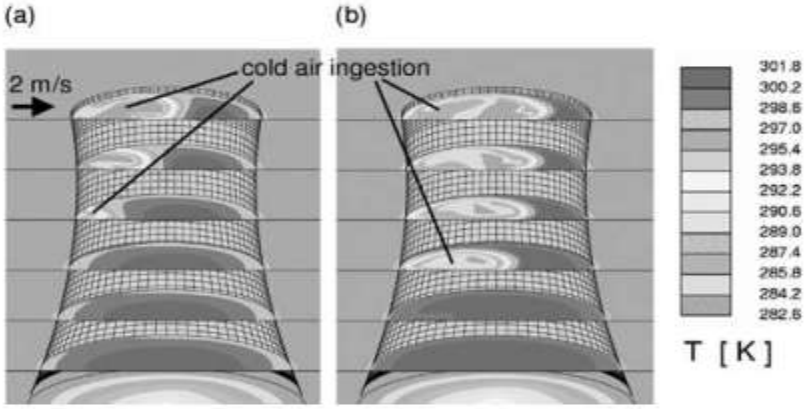

Figure 20: Temperature distribution (3D view) at indicated iteration steps, cross wind velocity 2 m/s, cooling tower without inner rim structure: (a) position 2 and (b) position 3.

At position 4 (Fig. 24d), the warm air fills the cooling tower completely but is still disturbed at the outlet. However, the curve for the cold water temperature in Fig. 20 shows that it has decreased now rapidly and will further decrease until a similar situation is reached as it has been at position 1. Then, the next cycle starts. Thus, the effect of cross wind for cooling tower design with significant deficiencies might lead to a timely periodic cold air ingestion as it has been shown by Figs. 17–19. However, it has to be taken into account that the results shown in Section 5.2 are only of limited numerical value as the calculation is not unsteady, but results are obtained of a periodic numeric instability in a steady calculation using a time-marching scheme. Unsteady calculations of the cold air ingestion phenomenon in case of a cross wind situation have not been performed now by the authors due to the enormous calculation efforts. With increased performance of modern PC-Clusters, this possibility should soon be in reach for validation of the observed and described phenomenon.

REFERENCES

[1]. Cooling Tower Performance Curves, Cooling Tower Institute: Houston, TX, 1967.
[2]. Kelly, N.W., Kelly's Handbook of Crossfl ow Cooling Tower Performance, Neil W. Kelly and Associates: Kansas City, MO, 1976.
[3]. Majumdar, A.K., Singhal, A.K. & Spalding, D.B., Numerical modeling of wet cooling towers – Part 1: Mathematical and physical models. Journal of Heat Transfer, 105, pp. 728–735, 1983.
[4]. Majumdar, A.K., Singhal, A.K., Reilly, H.E. & Spalding, D.B., Numerical modeling of wet cooling towers – Part 2: Application to natural and mechanical draft towers. Journal of Heat Transfer, 105, pp. 736–743, 1983.
[5]. Star-CD Version 3.20, CD adapco Group, 2004.
[6]. Poppe, M., Wärme- und Stoffübertragung bei der Verdunstungskühlung im Gegen- und Kreuzstrom (in German), PhD Thesis, Technical University of Hannover, 1972.
[7]. Beger, G., Modellversuche zur Windlastbestimmung an Kühltürmen in Gruppenaufstellung (in German). Energietechnik, 42(2), pp. 45–48, 1992.
[8]. Beger, G., Modelluntersuchungen der Strömungsverhältnisse im Kopfbereich von Naturzugkühltürmen (in German). Energietechnik, 40(4), pp. 135–139, 1990.